A new bio-optical algorithm for the remote sensing of algal blooms in complex ocean waters

Palanisamy Shanmugam[1]

Received 10 November 2010; revised 18 January 2011; accepted 24 January 2011; published 16 April 2011.

[1] A new bio-optical algorithm has been developed to provide accurate assessments of chlorophyll *a* (Chl *a*) concentration for detection and mapping of algal blooms from satellite data in optically complex waters, where the presence of suspended sediments and dissolved substances can interfere with phytoplankton signal and thus confound conventional band ratio algorithms. A global data set of concurrent measurements of pigment concentration and radiometric reflectance was compiled and used to develop this algorithm that uses the normalized water-leaving radiance ratios along with an algal bloom index (ABI) between three visible bands to determine Chl *a* concentrations. The algorithm is derived using Sea-viewing Wide Field-of-view Sensor bands, and it is subsequently tuned to be applicable to Moderate Resolution Imaging Spectroradiometer (MODIS)/Aqua data. When compared with large in situ data sets and satellite matchups in a variety of coastal and ocean waters the present algorithm makes good retrievals of the Chl *a* concentration and shows statistically significant improvement over current global algorithms (e.g., OC3 and OC4v4). An examination of the performance of these algorithms on several MODIS/Aqua images in complex waters of the Arabian Sea and west Florida shelf shows that the new algorithm provides a better means for detecting and differentiating algal blooms from other turbid features, whereas the OC3 algorithm has significant errors although yielding relatively consistent results in clear waters. These findings imply that, provided that an accurate atmospheric correction scheme is available to deal with complex waters, the current MODIS/Aqua, MERIS and OCM data could be extensively used for quantitative and operational monitoring of algal blooms in various regional and global waters.

Citation: Shanmugam, P. (2011), A new bio-optical algorithm for the remote sensing of algal blooms in complex ocean waters, *J. Geophys. Res.*, *116*, C04016, doi:10.1029/2010JC006796.

1. Introduction

[2] Increasing runoff of nutrient pollution, hydrographic changes and climate oscillations are a major cause of the global increase in massive microalgal blooms [*Anderson et al.*, 2002; *Sellner et al.*, 2003; *Carstensen et al.*, 2004; *Edwards et al.*, 2006], some of which threaten the diversity in a natural ecosystem and are unpalatable for commercially important shellfish in many coastal waters of the world [*Stumpf*, 2001; *Kirkpatrick et al.*, 2004; *Yentsch et al.*, 2008; *Shanmugam et al.*, 2008, and references therein]. This has prompted the decision to constitute a number of national, regional and international programs, namely the Global Ecology and Oceanography of Harmful Algal Blooms (GEOHAB) (http://ioc.unesco.org/hab/GEOHAB.htm), Northwest Pacific Action Plan (NOWPAP) (http://www.nowpap.org/), and Korean Harmful Algal Bloom Research Group (KORHAB) (http://ioc.unesco.org/hab/HAN29_Final_comp.pdf), to understand the features and mechanisms underlying the population dynamics of recent algal blooms events, and to improve and develop management and amelioration strategies [*Shanmugam et al.*, 2008].

[3] Remotely sensed ocean color data acquired with satellite sensors such as SeaWiFS (Sea-viewing Wide Field-of-view Sensor) and CZCS (Coastal Zone Color Scanner) have greatly increased our knowledge of the distribution of chlorophyll *a* in the oceans. They have been successfully used to provide a synoptic description of optical and biological properties of marine waters, to address marine environmental issues, and to investigate a variety of topics including marine primary productivity, ecosystem dynamics, sedimentation and pollution [*Steidinger and Haddad*, 1981; *Campbell and Esaias*, 1983; *Carder and Steward*, 1985; *Harding et al.*, 1992; *Behrenfeld and Falkowski*, 1997; *Bailey and Werdell*, 2006; *Marrari et al.*, 2006; *Volpe et al.*, 2007]. As evidenced by the successful use of these data to study pigment distributions, the abundance of phytoplankton pigments plays an important role in determining spectral sea

[1]Ocean Optics and Imaging Group, Department of Ocean Engineering, Indian Institute of Technology Madras, Chennai, India.

0148-0227/11/2010JC006796

surface reflectance. Particularly in coastal waters however, changes in ocean color are a result of in-water constituents such as the chlorophyll *a* (Chl *a*), suspended sediments (SS), and colored dissolved organic matter (CDOM), which possess different absorption and scattering properties [*Schofield et al.*, 1999; *Martin Traykovski and Sosi*, 2003]. Of these, Chl *a* is widely used as an index of phytoplankton biomass, and an important parameter in the bio-optical modeling studies to determine its absorption coefficient and further separate into different phytoplankton groups [*Cullen et al.*, 1997; *Carder et al.*, 1999; *Schofield et al.*, 2004]. Because ocean color signals vary in response to many factors and materials such as SS and CDOM often interfere with phytoplankton signal, it remains a challenge with conventional band ratio algorithms to accurately determine and differentiate chlorophyll *a* concentrations from other constituents in optically complex waters.

[4] Many global algorithms that have been developed to estimate Chl *a* concentrations from satellite ocean color data typically take advantage of decreased radiance (or reflectance) in the blue (440–510 nm) and increased radiance (or reflectance) in the green (550–565 nm) by working in terms of the ratios in these two wavelength domains (e.g., the SeaWiFS Ocean Chlorophyll four-band algorithm OC4v4 involving $\lambda 1 = 443$, 490, and 510 nm, and $\lambda 2 = 555$ nm), and Moderate Resolution Imaging Spectroradiometer (MODIS)/Aqua Ocean Chlorophyll three-band algorithm OC3 involving $\lambda 1 = 443$ and 488 nm, and $\lambda 2 = 551$ nm) [*O'Reilly et al.*, 1998, 2000]. While this approach has been valid in oceanic waters where a change in the concentration of Chl *a* mainly causes a shift in the blue to green ratios of upwelling light fields [*Morel and Prieur*, 1977], these ratios can vary in response to factors besides chlorophyll concentration, and therefore introduce large errors in pigment retrievals from satellite data in waters with high CDOM and SS contents [*Sathyendranath*, 2000; *Darecki and Stramski*, 2004]. It is worth noting that spectral curvature algorithms were developed and successfully applied to aircraft radiance data to investigate Chl *a* distributions in estuarine and coastal waters [*Campbell and Esaias*, 1983; *Harding et al.*, 1992]. These algorithms were found to have the potential to reduce uncertainty in Chl *a* retrievals in turbid waters. A number of other optical methods have been developed and used with satellite data to provide a valuable tool for detection and mapping of algal blooms [*Gower and Borstad*, 1990; *Stumpf*, 2001; *Subramaniam et al.*, 2001; *Tomlinson et al.*, 2004; *Hu et al.*, 2005; *Wynne et al.*, 2005; *Ahn and Shanmugam*, 2006; *Kutser et al.*, 2006; *Cannizzaro et al.*, 2008]. Such approaches are qualitative, regional, complex and/or inaccurate because of known atmospheric correction problems or high CDOM and SS contents in Case 2 waters, which require new algorithms based on new approaches dealing with both atmospheric correction and retrievals of ocean bio-optical properties from water-leaving radiance [*Ahn and Shanmugam*, 2007].

[5] Our objective is to develop a robust chlorophyll *a* algorithm for use with satellite observations to detect and monitor various algal blooms in complex ocean waters. The performance of this algorithm is evaluated using large in situ bio-optical data sets and satellite matchups from a variety of waters including oceanic and coastal environments. The new algorithm is also compared with OC3 and OC4v4 bio-optical algorithms using these data sets. Finally, its strength and weakness in differentiating algal blooms from other features is evaluated using MODIS/Aqua images over the Arabian Sea and west Florida shelf.

2. Data and Methods

2.1. In Situ Data Sets

[6] Five different data sets containing spectral measurements at key wavelengths and pigment concentrations from different regions around the world were used to develop and evaluate the new algorithm, namely (1) International Ocean Color Coordinating Group (IOCCG) in situ data set (N = 591, Chl *a* 0.03–32.65 mg m^{-3}), (2) Korean Ocean Research and Development Institute (KORDI) in situ data set (N = 57, Chl *a* 1.12–119.33 mg m^{-3}), (3) NASA bio-Optical Marine Algorithm Data (NOMAD) in situ data set (N = 2074, Chl *a* 0.019–48 mg m^{-3}), (4) NOMAD satellite matchups data set (N = 221, Chl *a* 0.04–43.2 mg m^{-3}), and (5) Carder in situ data set (N = 643, Chl *a* 0.02–125.2 mg m^{-3}). Of these, NOMAD and IOCCG data sets are global, high quality in situ bio-optical data sets collected over a wide range of optical properties, trophic status, and geographical locations in open ocean waters, estuaries, and coastal waters (including Arabian Sea and coastal waters of India). The KORDI data were collected in bloom waters of the Korean South Sea during August 2001, 2003 and 2004. The Carder data were collected during several cruises in west Florida shelf and neighboring waters in different seasons and years from 1999 to 2006. Only stations having both optical and pigments measurements were considered forming the above data sets. The first two data sets were used for algorithm development, while the later three independent data sets were used for algorithm validation/performance assessment. Using these data sets, the new algorithm was compared with OC3 and OC4v4 bio-optical algorithms developed for MODIS and SeaWiFS sensors. Briefly, the OC3 algorithm estimates Chl *a* from a cubic polynomial formulation by using the maximum band ratio determined as the greater of the $R_{rs}(443)/R_{rs}(551)$ or $R_{rs}(488)/R_{rs}(551)$, whereas the OC4v4 algorithm estimates Chl *a* from a fourth-order polynomial (five coefficients) by using the maximum band ratio determined as the greater of the $R_{rs}(443)/R_{rs}(555)$, $R_{rs}(490)/R_{rs}(555)$, or $R_{rs}(510)/R_{rs}(555)$ values [*O'Reilly et al.*, 1998, 2000]. These algorithms are presently used for routine global processing of SeaWiFS and MODIS imagery.

[7] One of these three independent validation data sets (i.e., NOMAD satellite matchups) that contains matchups of the SeaWiFS determinations of reflectance spectra $R_{rs}(0^+, \lambda)$ and collocated field observations was used to validate the accuracy of our algorithm when applied to satellite imagery. Since some of these reflectance spectra from SeaWiFS measurements that were not quality controlled by excluding observations where the atmospheric correction may be suspect had negative values at short wave bands (412 and 443 nm), it was necessary to use a Case 2 water correction scheme (CCS) [*Shanmugam*, 2010] to correct the negatively biased data sets. This scheme is flexible to deal with such cases and produces accurate water-leaving radiances suitable for algorithm implementation in complex waters. The ulti-

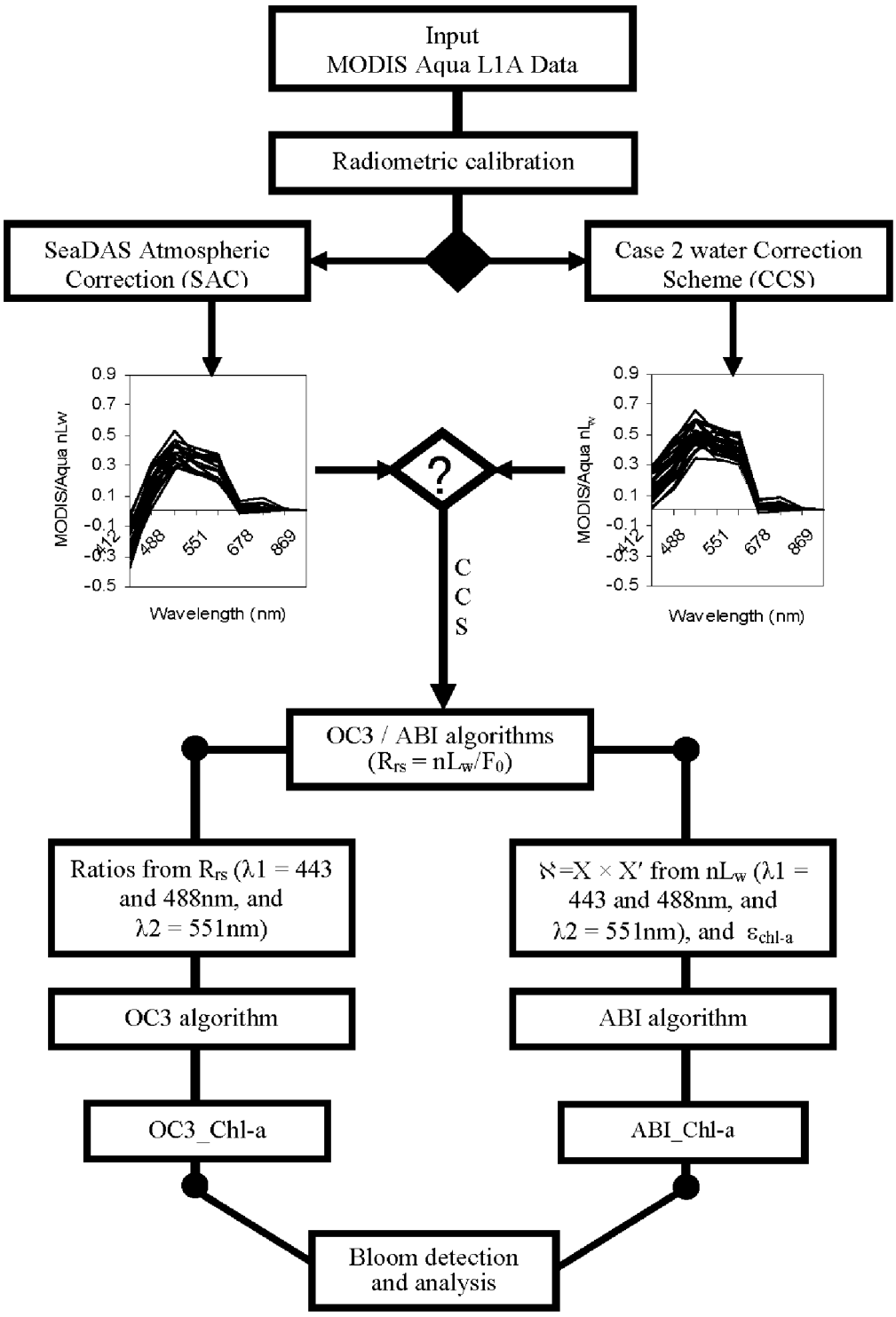

Figure 1. Schematic representation of the algorithm implementation to Moderate Resolution Imaging Spectroradiometer (MODIS)/Aqua imagery.

mate goal of using such large data sets in combination with the CCS was to evaluate the extent to which the new algorithm could be applied to satellite ocean color data (such as MODIS, MERIS (Medium Resolution Imaging Spectrometer), and OCM (Ocean Color Monitor OCM)) to estimate Chl *a* and use it for detection and mapping of algal blooms in various regional and global waters.

2.2. Satellite Data

[8] High-resolution MODIS/Aqua Level 1A (~1 km/pixel at nadir, LAC-local area coverage) data over the Arabian Sea and west Florida shelf in different periods (9 September 2003, 25 April 2005, 05 October 2006, and 18 February 2010) were obtained from NASA Goddard Space Flight Centre (http://oceancolor.gsfc.nasa.gov/) and processed up

to Level 2 (L2) to obtain remote sensing reflectance and normalized water-leaving radiance (nL_w) for the visible bands (412, 443, 488, 531, 551 nm) using SeaDAS integrated with the CCS scheme. Because these two regions are typical examples of nearshore high-productivity waters and coastal/estuarine waters dominated by algal blooms and suspended sediments [*Desa et al.*, 2001; *Tang et al.*, 2002; *Gomes et al.*, 2008; *Hu et al.*, 2005; *Cannizzaro et al.*, 2009], the standard atmospheric correction algorithm (with SeaDAS) applied to L1A raw data resulted in biased low and often negative reflectance values in these waters. This problem is essentially caused by the NIR ocean contributions in such waters [*Siegel et al.*, 2000; *Wang and Shi*, 2005]. Thus, the MODIS/Aqua data were processed using the combined CCS and SeaDAS atmospheric algorithm in order to derive accurate normalized water-leaving radiances (Figure 1). These data were further processed using the new algorithm and OC3 algorithm to derive the Chl *a* concentrations. In addition, reflectances at the wavelengths of 412, 488 and 531 nm were used to generate true color composite images for characterizing different levels of algal accumulation and distinguishing different water types in the study area.

3. Algorithm Description

[9] The ocean color signal sensed by a satellite can be quantified using the remote sensing reflectance just above the sea surface R_{rs} (0^+, λ) and is defined as the ratio of upwelling radiance (L_w (0^+, λ)) to downwelling irradiance E_d (0^+, λ) just above the sea surface. Both these parameters may be obtained after extrapolation of radiance and irradiance measured just below the sea surface and their ratio can be further related to the inherent optical properties (IOPs) of the water column via the relation of *Mobley* [1994],

$$R_{rs}(0^+,\lambda) = \frac{L_w(0^+,\lambda)}{E_d(0^+,\lambda)} \approx \frac{1-r}{n^2}\frac{L_u(0^-,\lambda)}{E_d(0^-,\lambda)} \approx k\left(\frac{f}{Q}\right)\left(\frac{b_b(\lambda)}{b_b(\lambda)+a(\lambda)}\right) \quad (1)$$

where r is the average specular reflectance at the sea surface, ~3% *Austin* [1974], n is the index of refraction of seawater (1.341), L_u (0^-, λ) is the spectral upwelling radiance just below the sea surface measured by a profiling spectroradiometer, E_d (0^-, λ) is the incident spectral irradiance just below the sea surface measured by a similar radiometer, $a(\lambda)$ and $b_b(\lambda)$ are the IOPs (absorption and backscattering coefficients, respectively), f/Q is a factor accounting for the bidirectional structure of the upward radiance field (≈0.0949), and k (≈0.54) accounts for the transmission and reflection of the air-sea interface [*Mobley*, 1994; *Siegel et al.*, 1995; *Gordon et al.*, 1988]. Remote sensing reflectance is the standard input to many of the derived product algorithms and is converted to normalized water-leaving radiance nL_w (λ) as follows,

$$nL_w(\lambda) = F_0(\lambda) \times R_{rs}(\lambda) \quad (2)$$

where F_0 is mean solar irradiance at wavelength λ. nL_w (λ) is more stable than the water-leaving radiance spectra used for the algorithm development [*Ahn and Shanmugam*, 2006].

[10] The algal bloom index (ABI) originally developed by *Ahn and Shanmugam* [2006] is calculated based on the normalized water-leaving radiance at three wavelengths in the visible domain (i.e., 443, 490, 555 nm), as follows,

$$X = ABI = 10^{\left[\left(\frac{nL_w(490)}{nL_w(555)}\right)-\left(\frac{nL_w(443)}{\alpha}\right)\right]/\left[\left(\frac{nL_w(490)}{nL_w(555)}\right)+\left(\frac{nL_w(443)}{\alpha}\right)\right]} \quad (3)$$

where the threshold value of α is assumed unity, which allows the calculation to work well as phytoplankton absorption is the important driver of reflectance in the blue (443 nm), and other factors regulate reflectance at 555 nm (thus, Chl *a* has a strong, inverse relationship with the reflectance at 443 nm and a much weaker, positive relationship at 555 nm [*Kostadinov et al.*, 2007]). X is the algal bloom index (ABI) which varies from 0 to 10. An index value of 0 means no algal bloom and close to 10 indicates the highest possible of algal bloom in a given location. Note that the denominator of equation (3) from the combined ratios of $nL_w(490)/nL_w(555)$ and $nL_w(443)/\alpha$ is relatively much larger (as $nL_w(443)/\alpha$ is maximal) than the numerator of equation (3) from the difference of these ratios for clear and turbid waters (nonblooms), which result in lower index values for these waters. In contrast, both the denominator and numerator of equation (3) become small (as $nL_w(443)/\alpha$ is minimal) and are close with each other, this result in higher index values for waters containing algal blooms. As a result, the ABI should be maximally sensitive to bloom variability and minimally to materials other than phytoplankton such as SS and CDOM in typical Case 2 waters. The ABI can be used to differentiate pixels with microalgae from those with clear open oceans and turbid waters. It also makes certain that the ABI is more accurate than that of a single band water-leaving radiance ($L_w(443)$) using a cubic polynomial equation [*Ahn and Shanmugam*, 2006]. Furthermore, the use of nL_w (instead of L_w) can better represent the spectral changes of algal blooms in the visible bands.

[11] Since the ABI has a restricted range of values (0–10) that cannot explain a wide range of Chl *a* variability, it is multiplied by a variable X′ involving two conventional nL_w ratios (commonly used in the standard bio-optical algorithms, e.g., OC3 and OC4v4) to modify the amplitude of these ratios in order to reduce uncertainties in Chl *a* retrievals. This variable factor is quite similar to that used in the spectral curvature algorithm that was applied to aircraft radiance data in turbid water effectively [*Campbell and Esaias*, 1983; *Harding et al.*, 1992]. It decreases with increasing Chl *a* concentrations and is defined as follows,

$$\left.\begin{array}{l} \aleph = X \times X' \\ \text{where, } X' = \left(\frac{(nL_w(443)\times nL_w(490)/nL_w(555))^2}{(\lambda_{490}-\lambda_{443})}\right) \end{array}\right\} \quad (4)$$

Similar to other empirical approaches [*O'Reilly et al.*, 1998], large in situ measurements are used to relate the $\aleph = X \times X'$ to Chl *a* concentrations. This relation is different from those of the conventional ratio approaches since the basis for the development of these algorithms has been the observation that changes in Chl *a* in Case 1 waters [*Morel and Prieur*, 1977] are accompanied by more or less systematic variations in the ocean optical properties including the spectrum of ocean reflectance [*Gordon and Morel*, 1983]. In Case 2 waters, these ratios are significantly influenced by materials

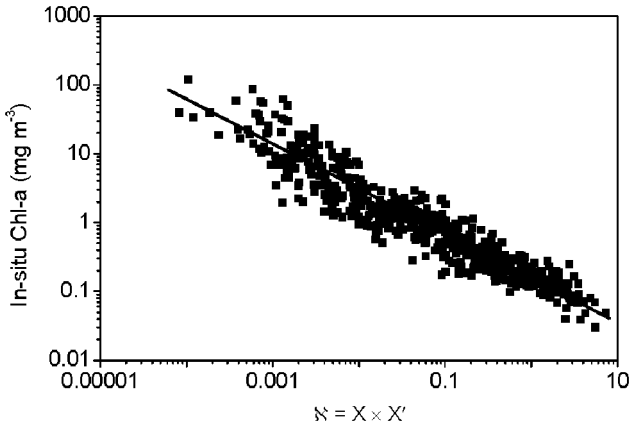

Figure 2. In situ chlorophyll *a* concentration versus $\aleph = X \times X'$ (using International Ocean Color Coordinating Group (IOCCG) and Korean Ocean Research and Development Institute (KORDI) in situ data sets). Solid line is the best fit regression to our data (N = 648, $R^2 = 0.90$).

other than phytoplankton such as the CDOM, SS and perhaps bottom reflectance [*Siegel et al.*, 2000; *Darecki and Stramski*, 2004; *Bailey and Werdell*, 2006].

[12] Figure 2 shows the relationship between $\aleph = X \times X'$ and Chl *a* concentrations that provides the best representation for the most of data collected in a wide variety of waters. A tight inverse correlation between these two parameters is observed ($R^2 = 0.90$). We fitted the data of Chl *a* versus $\aleph = X \times X'$ to the power function

$$\varepsilon_{chl-a} = 0.1403 \times (\aleph)^{(-0.572)} \tag{5}$$

where ε_{chl-a} is the initial estimate of Chl *a* concentration constrained to similar optical regimes from where the large in situ data were collected and used to derive the above relationship. To make this relationship applicable in a wide range of water types and to be well-suited for use with MODIS/Aqua data, it is further tuned to correlate ε_{chl-a} to ABI_ Chl *a* products;

$$ABI\_Chl-a = 125 \frac{\varepsilon_{chl-a}^{1.056}}{\left(126.69 + \varepsilon_{chl-a}^{1.056}\right)^{0.96}} \tag{6}$$

The coefficients for the ABI_ Chl *a* were locally optimized using the same data sets (as in equation (5)) in order to minimize uncertainties in Chl *a* retrievals. Though the ABI algorithm is developed for marine environments, it can be extended to the inland water bodies (such as inland Lakes) after fine tuning instead of reparameterization of the algorithm. However, this requires an understanding of the specific optical properties of such environments.

4. Evaluation of Algorithm Accuracy

[13] The accuracy of the ABI and standard algorithms was assessed (for three independent data sets such as NOMAD in situ data set, NOMAD-SeaWiFS matchups, and Carder data sets) by comparing their predicted Chl *a* values with those measured in the laboratory. The comparison was quantified by means of the difference between predicted Chl *a* and measured Chl *a*. Systematic and random errors were characterized by the mean relative error (MRE) and root mean square error (RMSE), respectively [*Lee*, 2006]; these metrics are defined as:

$$MRE = \sum_{i=1}^{N} \frac{\log\left(Chl\ a_i^{predicted}\right) - \log\left(Chl\ a_i^{insitu}\right)}{\log\left(Chl\ a_i^{insitu}\right)} \times 100 \tag{7}$$

$$RMSE = \left(\frac{\sum_{i=1}^{N} \left[\log\left(Chl\ a_i^{predicted}\right) - \log\left(Chl\ a_i^{insitu}\right)\right]^2}{N - 2} \right)^{1/2} \tag{8}$$

where N is the number of valid retrievals. The MRE is a bias estimator and has been widely used in the recent investigations [e.g., *Darecki and Stramski*, 2004, and references therein]. These errors were calculated after log transformation. The accuracy of Chl *a* predictions (for all data acquired) was also assessed based on the slope, intercept and correlation coefficient of the $Chl-a^{predicted} - Chl-a^{insitu}$ relationships [*IOCCG*, 2006]. Table 1 summarizes the results of algorithm validation for all the three data sets.

5. Results

5.1. Algorithm Validation

[14] The performance of the ABI algorithm was evaluated using three independent data sets: Carder in situ data set, NOMAD in situ data set and NOMAD-SeaWiFS matchups, and by comparison with the standard algorithms such as OC3 and OC4v4. Figure 3 compares the algorithm estimates of Chl *a* with in situ measurements of Chl *a* concentration. The results of algorithm performance evaluation are summarized in Table 1. To gain further insight into the difference between the algorithm estimates and in situ measurements of Chl *a* at each station/location, the absolute relative difference/error (AMRE) was calculated and plotted as a function of in situ Chl *a* (Figures 3d–3f). Note that, for all three data sets, ABI_ Chl *a* concentrations are closely consistent with in situ Chl *a* across a wide range of environments and are

Table 1. Comparison of Algorithm Performances Using the Three Independent Data Sets

Algorithms	MRE[a] (%)	RMSE[a]	Intercept	Slope	R^2	N
Carder In Situ Data Set						
ABI	−17.44	0.2366	−0.0859	0.9461	0.8668	643
OC3	−52.81	0.3105	−0.2127	0.9706	0.8560	643
OC4	−38.53	0.3068	−0.1830	0.8683	0.8466	643
NOMAD In Situ Data Set[b]						
ABI	40.06	0.2723	0.0735	1.0601	0.8190	2074
OC3	−6.75	0.2677	0.0060	1.1149	0.8148	2074
OC4	25.14	0.2658	0.0404	1.0118	0.8271	2074
NOMAD SeaWiFS-Matchups Data Set						
ABI	−17.97	0.2110	−0.0461	0.9946	0.8714	221
OC3	−57.68	0.2523	−0.1442	1.0033	0.8689	221
OC4	−37.67	0.2348	−0.1046	0.9350	0.8709	221

[a]MRE, mean relative error; RMSE, root mean square error.
[b]NOMAD, NASA bio-Optical Marine Algorithm Data.

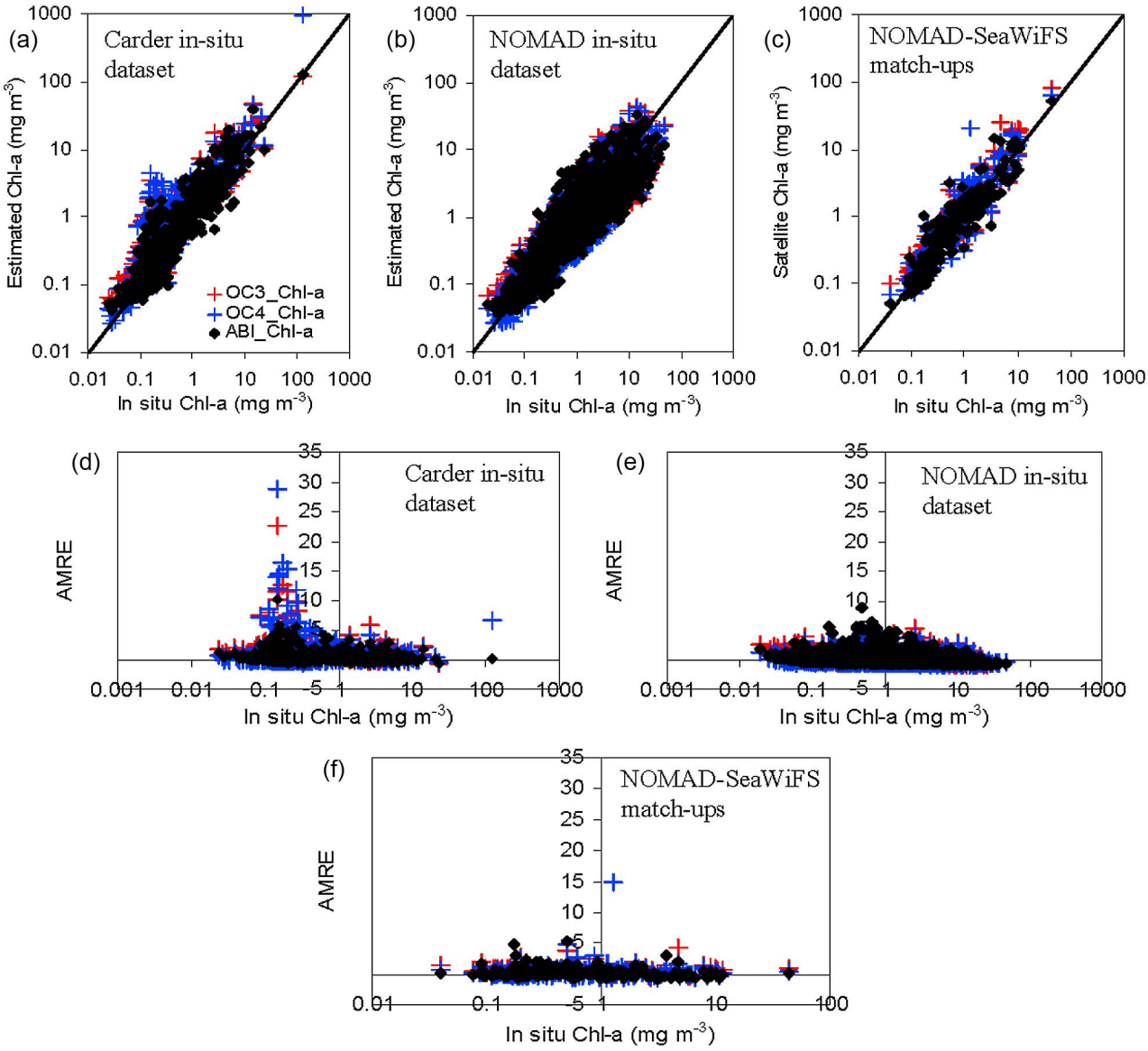

Figure 3. Scatterplots illustrating the comparisons of estimated Chl *a* concentrations to in situ Chl *a* concentrations for the (a) Carder and (b) NASA bio-Optical Marine Algorithm Data (NOMAD) in situ data sets and (c) NOMAD-SeaWiFS matchups. The solid lines represent the 1:1 lines. (d–f) The absolute mean relative error (AMRE = estimated Chl *a*− in situ Chl *a*/in situ Chl *a*) versus in situ Chl *a* concentrations across a wide range of waters is also shown.

generally comparable with those of the OC3 and OC4v4 algorithms. It exhibits consistently good correlations with in situ Chl *a* concentrations, with R^2 always greater than 0.80. For the Carder data set, the ABI algorithm performs generally better than OC3 and OC4v4 algorithms, but its slope is slightly lower than that for the OC3 algorithm. Notably, all other statistics have improved for the ABI algorithm. The OC4v4 algorithm performs only marginally better than OC3, but it has slightly lower slope and R^2 values. MRE has considerably deteriorated for OC3 (as the OC4v4 algorithm). Looking more closely at the AMRE, both OC3 and OC4 algorithms significantly overestimate Chl *a*, especially for open ocean waters and regions with Chl *a* < 0.5 mg m^{-3}. These results are consistent with the previous observations of systematic overestimation of Chl *a* in waters with low Chl *a* values [*Stramska et al.*, 2003; *Pan et al.*, 2008]. On the contrary, the overestimation is significantly reduced by the ABI algorithm in low and high Chl *a* regimes. This demonstrates successful retrieval of Chl *a* concentrations within a reasonable accuracy, and shows significant improvements over the OC3 and OC4v4 algorithms. When extending a similar validation with NOMAD in situ data set consisting of large bio-optical measurements in a diverse range of environments, the ABI algorithm performs roughly equal compared with OC3 and OC4v4 algorithms (considering RMSE, slope and R^2 in Table 1). However, its MRE is considerably worse. The OC3 algorithm performs slightly better than OC4v4, but has achieved excellent MRE and

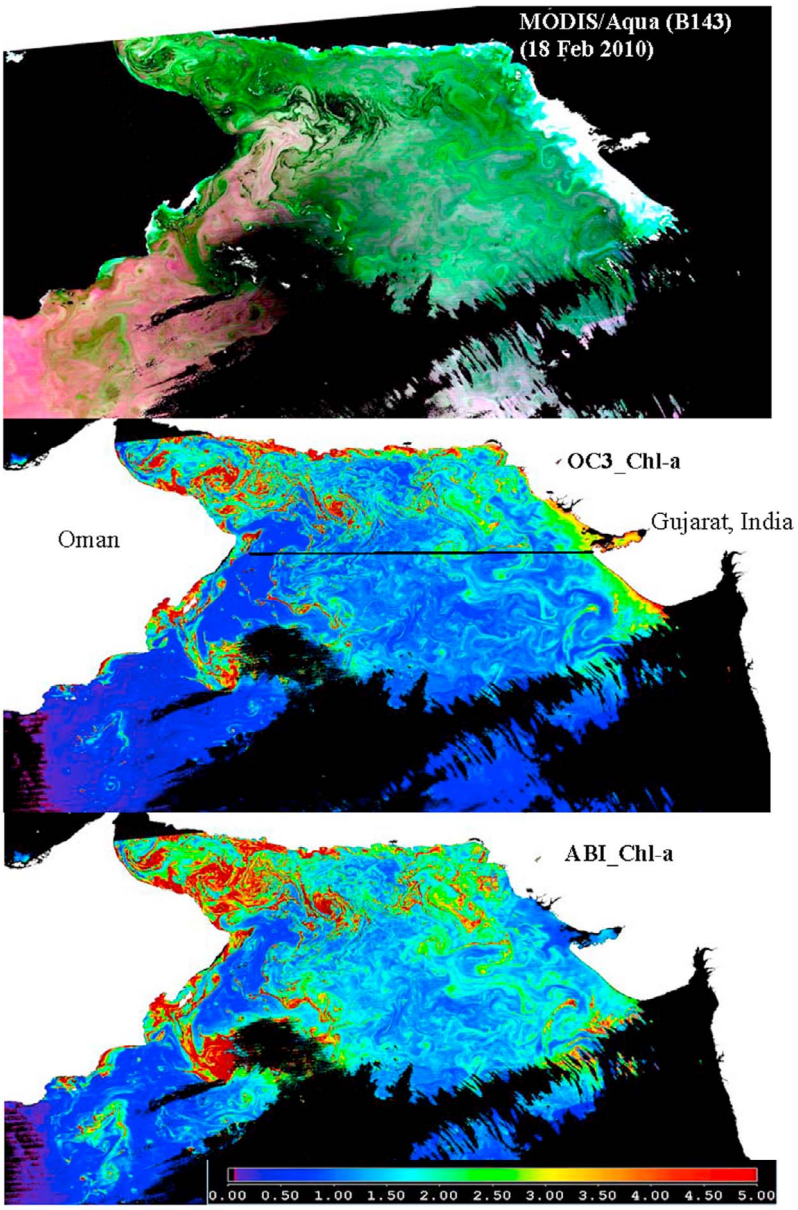

Figure 4. (top) A MODIS/Aqua true color composite on 18 February 2010 in the Arabian Sea and Gulf of Oman. The corresponding Chl *a* images derived using (middle) the OC3 and (bottom) ABI algorithms. The combined SeaDAS algorithm and CCS scheme was used for atmospheric correction of MODIS/Aqua data.

intercept values. Note that all three algorithms show similar AMRE values closely aligned between the no-bias line (baseline), albeit with slight underestimations across the entire range of Chl *a* concentrations. A closer inspection also allows us to identify few data points above the baseline indicating an overestimation of Chl *a* by the ABI algorithm in waters with Chl *a* 0.1–1 mg m^{-3}, however this is not the same magnitude as previously observed with the OC3 and OC4 algorithms.

[15] In order to validate the products derived from ocean color sensors, it is imperative to compare in situ measurements of Chl *a* with remotely sensed values. Here, an independent data set containing matchups (N = 221) of the SeaWiFS determinations of reflectance $R_{rs}(\lambda)$ and collocated in situ Chl *a* observations was used to assess the performance of the ABI and standard algorithms. When applied to the SeaWiFS data sets, Chl *a* retrievals with the ABI algorithm are substantially improved as compared to those with the OC3 and OC4v4 algorithms. Contrary to previous validation, OC4v4 performs marginally better than OC3 algorithm depending on the statistics considered. For example, OC4v4 has better MRE, RMSE, intercept and R^2 values, but other statistics are better for OC3 algorithm. For Chl *a* matchups (Figures 3c and 3f), both the OC3 and OC4v4 algorithms show noticeable overestimations (at the higher and lower end) with respect to in situ measurements in clear oceanic and coastal waters, although their retrievals being comparable with in situ data in waters with moderate

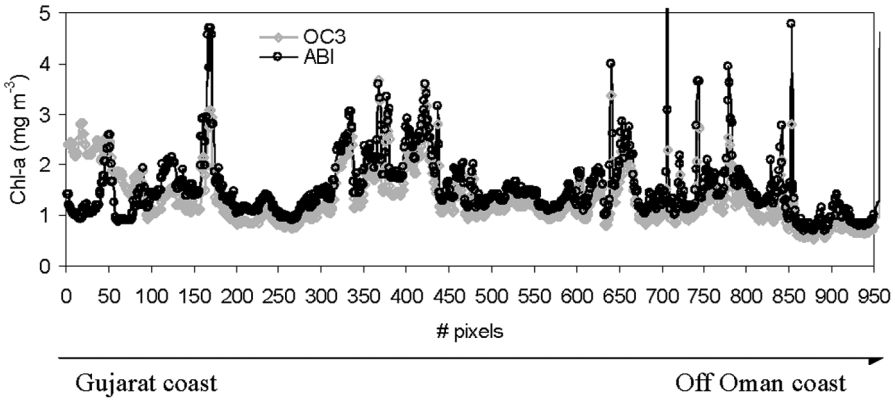

Figure 5. The profiles of MODIS/Aqua OC3_ Chl *a* and ABI_ Chl *a* from a transect (east-west transect in Figure 4, middle) running across the bloom from turbid coastal areas of the eastern Arabian Sea (Gujarat, India) to relatively clear waters of the western Arabian Sea (Oman).

Chl *a* concentrations. By contrast, the validation matchups between in situ Chl *a* and satellite Chl *a* from ABI algorithm are very excellent and demonstrate good agreement (i.e., bias <18%, which is above the accuracy goal of 35% for satellite retrieved Chl *a* estimates [*Garcia et al.*, 2005]). Also, its AMRE has improved considerably over previous validations. The best statistics with less errors of the validation satellite matchups imply that the ABI algorithm has potential to not only improve Chl *a* retrievals in clear oceanic waters but also reliably retrieve this component in optically complex environments when applied to satellite data along with a Case 2 water correction scheme.

5.2. Application to Satellite Data in Complex Waters

[16] To investigate the performance of the ABI and OC3 algorithms in optically complex waters (highly turbid and extensive bloom waters), the high-resolution MODIS/aqua images acquired over the Arabian Sea and west Florida shelf were used. These two regions are among the most productive and turbid regions in the global oceans [*Desa et al.*, 2001; *Joint Global Ocean Flux Study*, 2002; *Chauhan et al.*, 2002; *Tang et al.*, 2002; *Anderson et al.*, 2005; *Goes et al.*, 2005; *Walsh et al.*, 2006; *Brand and Compton*, 2007; *Emmett Duffy*, 2011]. The MODIS/Aqua image of the Arabian Sea acquired on 18 February 2010 is a good example of the spatially extensive green blooms of *Noctiluca miliaris*, and therefore used for evaluating the ABI and OC3 algorithms. Preliminary examination of true color MODIS/Aqua imagery from 18 February 2010 (Figure 4, top) reveals the predominant color of the ocean in coastal and offshore waters of the Arabian Sea, i.e., green to bluish green indicative of highly persistent and probably largest *N. miliaris* blooms of the year 2010 (http://earthobservatory.nasa.gov/images/imagerecords/43000/43050/ArabianSea_AMO_2010049_lrg.jpg). This true color image is highly comprehensive suggesting that large-scale *N. miliaris* blooms developed in the Gulf of Oman and mesoscale eddies that populated the western Arabian Sea during the winter monsoon and contributed to the genesis and dispersal of these blooms from the Gulf of Oman into the central Arabian Sea [*Gomes et al.*, 2008]. The green features in the nearshore and offshore waters are well characterized by much weaker radiances in the blue wavelength band, while the brighter features relate to highly reflective materials along the coastal areas (especially Gujarat in the eastern Arabian Sea) caused by strong radiance in the green wavelength band. These episodic high values of radiance in the green are indicative of high particle loads supporting its use as a plume indicator with satellite data sets [*Otero and Siegel*, 2004].

[17] Figures 4 (middle) and 4 (bottom) provides comparisons of Chl *a* concentrations for this region derived using the ABI and OC3 algorithms. Note that the OC3_ Chl *a* concentrations appear to be more realistic for open ocean waters than for coastal waters (especially along the Gujarat coast of India), where Chl *a* retrievals are considerably deteriorated (overestimated) and therefore not allowing to distinguish algal blooms from other features. This suggests that the significant contribution of suspended sediments and CDOM absorption may pose complications for applying global operational algorithms (e.g., OC4v4 and OC3) [*O'Reilly et al.*, 1998, 2000] to these complex coastal regions [*Desa et al.*, 2001; *Chauhan et al.*, 2002; *Pan et al.*, 2008]. However, the resulting image from ABI algorithm shows that it has definitely achieved a substantial improvement over the band ratio algorithm in both coastal and open ocean waters. As evident, ABI_ Chl *a* values are relatively low in bright coastal waters of Gujarat, but increase with increasing concentrations of green algae from coastal waters to offshore of the Arabian Sea. There is also a close agreement between algal patches observed on the true color image and those detected by the ABI algorithm (Figures 4, top and 4, bottom). It implies that the relative difference between the ABI algorithm and global algorithm would be relatively small in offshore regions (except intense blooms) and large in nearshore regions. This is because the spatial distribution and magnitude of Chl *a* from ABI algorithm displayed nearly similar trends with those of the OC3 algorithm in offshore regions, whereas in nearshore waters the ABI algorithm significantly reduced overestimation of Chl *a* by the OC3 algorithm (Figures 4, middle; 4, bottom; and 5).

[18] To support the full utility of the new algorithm, the Aqua-MODIS data (9 September 2003, 25 April 2005, and 5 October 2006) over west Florida shelf (WFS) waters were obtained from NASA Goddard Space Flight Centre and processed using the ABI and OC3 algorithms. Shown in Figure 6 are the results of ABI and OC3 algorithms in the

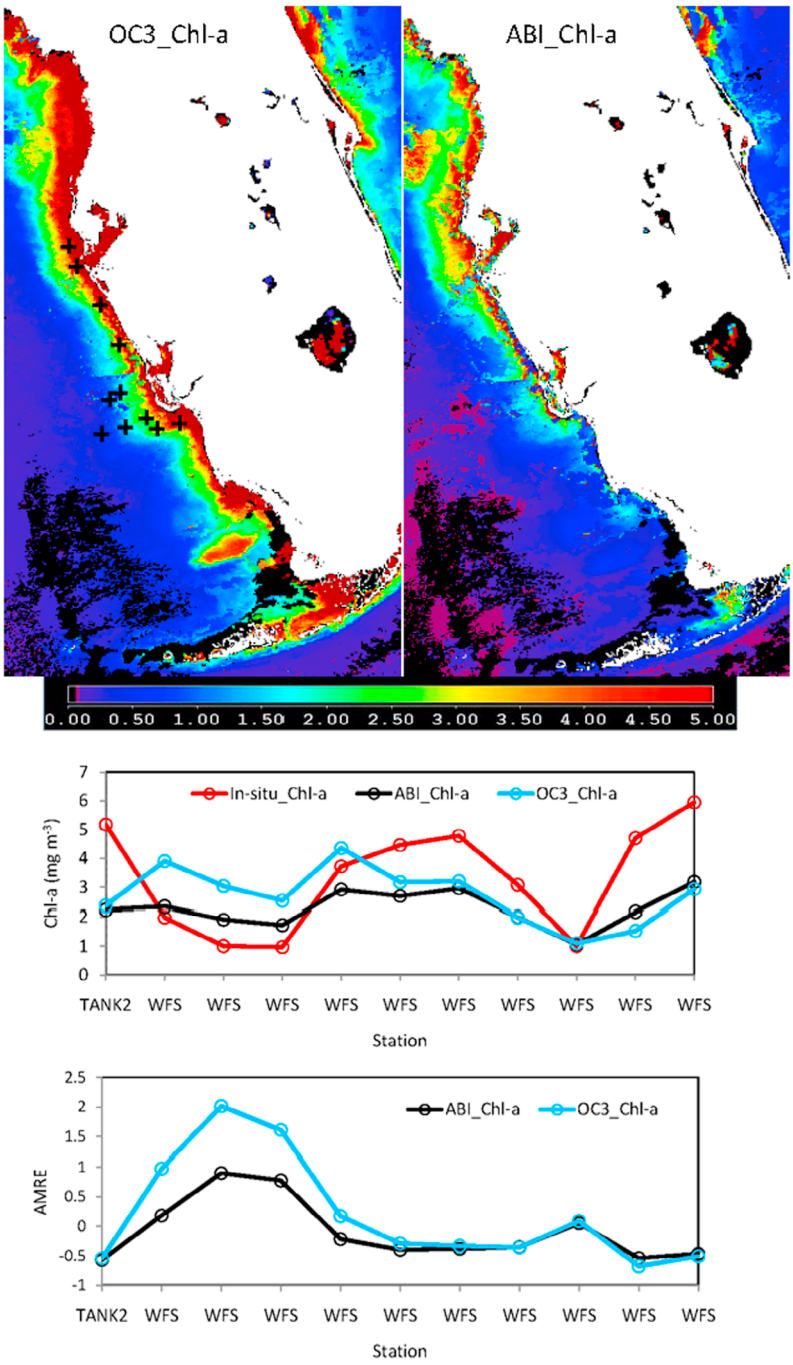

Figure 6. (top) Composite MODIS/Aqua Chl *a* (9 September 2003, 25 April 2005, and 5 October 2006) for the west Florida shelf (WFS) derived using the ABI and OC3 algorithms. (middle) Comparison of the algorithm-derived Chl *a* concentrations (from individual MODIS data) with in situ Chl *a* at discrete locations (station marks shown in the OC3-Chl *a* image) and (bottom) their absolute mean relative errors.

WFS region including Florida Keys. It is apparent that the OC3 algorithm exhibited continuous high pigment patches (likely because of overestimation) unrelated to algal blooms along the entire west coast of Florida (including Florida Keys, an area caused by high turbidity), which masked the contrast between dark and bright water features because all color changes are interpreted by the band ratio algorithm as changes in "chlorophyll *a* concentration" [*Hu et al.*, 2005]. In contrast, the ABI algorithm was found to easily differentiate between algal bloom and shallow water features, as it produced accurate Chl *a* retrievals with high values in truly bloomed waters and relatively low values in highly scattering waters. These predicted high pigment patches were found increasingly detached from other suspicious features and confirmed the visual analysis performed on the true color composite image.

[19] To better illustrate the accuracy of these algorithms, OC3_ Chl *a* and ABI_ Chl *a* products were compared with in situ Chl *a* (Carder data set) in coastal waters from Charlotte Harbor to Tampa Bay (Figures 6, middle and 6, bottom). As noted earlier, the OC3 algorithm tends to have overestimated Chl *a* at coastal stations (turbid/black waters) and underestimated at stations with high pigment contents. This resulted in high AMRE (−0.5~2) with OC3_ Chl *a*. On the contrary, the ABI algorithm reduced errors in coastal waters and performed marginally better than OC3 at other sites. The AMRE for ABI_ Chl *a* was better (−0.55~0.89) than that for OC3_ Chl *a* at most stations.

6. Discussion and Conclusions

[20] In the global perspective, green, red, brown or other microalgae blooms have been reported in many coastal oceans. The appearance, persistence and epidemic of some of these algal blooms have also been reported to cause fish mortality, shellfish poisoning, physiological impairment, and numerous ecological and health impacts [*Shanmugam et al.*, 2008, and references therein]. To quantitatively assess these blooms, many recent studies have relied on Chl *a* concentration to characterize their intensity, spatial distribution, seasonal and interannual variations. In this study, a new bio-optical algorithm (ABI) has been developed based on a large in situ data set for accurately assessing Chl *a* concentrations and mapping algal blooms in complex ocean waters. The performance of this algorithm has been evaluated with independent regional and global in situ data sets, SeaWiFS/MODIS matchups and MODIS/Aqua imagery. Its performance has also been assessed by comparison with the standard algorithms (i.e., OC3 and OC4). Importantly, our analyses showed that although the OC3 and OC4 algorithms reliably estimate Chl *a* concentrations in clear waters, they do not provide accurate absolute assessments of chlorophyll *a* concentration in optically complex waters. This was apparent in the MODIS/Aqua images that showed significant overestimation of Chl *a* with OC3 algorithm in coastal and offshore waters dominated by sediments and algal blooms. Using such Chl *a* data alone for analysis of nearshore areas with higher Chl *a* concentration further requires access to field data and interpretation by an analyst with an understanding of the chlorophyll *a* and optical patterns in the region. One potential reason is inherent limitations in the algorithm itself rather than the data set used to develop this band ratio algorithm. Previous studies have indicated that conventional band ratios are sensitive to other substances not covarying with Chl *a* [*Darecki and Stramski*, 2004; *Volpe et al.*, 2007; *Shanmugam et al.*, 2008, and references therein] and their ability to differentiate algal blooms from nonblooms and turbid features are therefore greatly reduced in complex waters. Inaccurate Chl *a* estimations from these ratios consequently prevent modeling studies to fully characterize the biogeochemical properties, especially in waters where CDOM and SS often overwhelm phytoplankton in the contribution to bio-optical properties [*Gordon and Morel*, 1983; *Kirk*, 1994; *Mobley*, 1994; *IOCCG*, 2006]. On the contrary, the ABI algorithm enabled reliable Chl *a* predictions when applied to both in situ and satellite data sets. Improved estimates of Chl *a* from the ABI algorithm helped the delineation and discrimination of algal blooms from other features in the Arabian Sea and west Florida shelf. Unlike the standard algorithms, the absolute values of reflectance are important for the ABI algorithm, and observational errors in the reflectance measurements and calculation will deteriorate the resulting data quality. Other sources of uncertainty in the new algorithm might stem from seasonal variability (riverine discharge along with wind forcing and direction) in the amount of Chl *a* caused by pigment package effect [*Bricaud et al.*, 1998; *Babin et al.*, 2003]. In addition to these, the degree of colony shelf-shading consequently alters the remote sensing reflectance spectrum for a given abundance [*Westberry et al.*, 2005].

[21] It is important to mention that many coastal regions contain some of the most consistently highly turbid or highly productive (phytoplankton blooms) waters; therefore significant water contributions at the longer wavelengths can be expected in these regions. The current SeaDAS atmospheric correction algorithm for producing the global ocean color product from SeaWiFS and MODIS uses the algorithm of *Gordon and Wang* [1994]. Specifically, the algorithm uses two near infrared (NIR) bands centered at MODIS 748 and 869 nm (SeaWiFS 765 and 865 nm) to determine aerosol type and estimate the atmospheric effects in the visible by extrapolating the aerosol effect from the NIR into visible bands. Though the basic assumption of negligible water-leaving radiance (L_w) in the NIR for deriving aerosol properties was replaced by *Stumpf et al.* [2003] and then updated by *Bailey et al.* [2010], the standard atmospheric correction algorithm still produces low or negatively biased L_w at short wavelengths in turbid and bloom-dominated waters (as found in the Arabian Sea). As a result, the ocean color products, such as Chl *a* concentration, have significant errors in these waters. Recently, it has been demonstrated that the coastal correction scheme (CCS) can be combined with standard SeaDAS atmospheric correction algorithm to derive improved ocean color products for the coastal turbid and productive waters [*Shanmugam*, 2010]. Thus, it was necessary to use this scheme to process the MODIS ocean color data for deriving accurate normalized water-leaving radiance and thereby improving ocean color products in the complex waters considered in this study. This approach allows pixels even with $L_w(412) < 0.2$ mW cm^{-2} μm^{-1} sr^{-1} that are excluded to minimize the impacts from atmospheric overcorrection in causing negative or significantly reduced water-leaving radiance [*Siegel et al.*, 2002] to become valid with positive water-leaving radiance values for these regions.

[22] In conclusion, a new algorithm has been developed as a potential tool for applications to data collected from spaceborne satellite ocean color sensors. Figure 1 provides simple guidelines on how to apply the algorithm. With the free availability of MODIS/Aqua data, the proposed algorithm has been tested on several MODIS/Aqua images and its effectiveness has demonstrated great potentials in accurately estimating Chl *a* concentrations and thus detecting and differentiating algal blooms from other features in the Arabian Sea and west Florida shelf. Establishment of such accurate records of Chl *a* and algal blooms is highly desired by the scientific community to understand local environmental changes in response to anthropogenic activities and global climate change. With in situ hydrographic, nutrients and bloom observations data, such records can addresses several questions: Why, when and where the summer HABs

develop, occur and terminate? Whether there is existence of any new bloom which had not been detected earlier by conventional field and remote sensing techniques? What are the spatial and temporal distributions of summer HABs? Can outbreaks be tied to the transport of offshore waters?, and, if so, can this transport be detected by remote sensing? What mechanisms elucidate the observed patterns? Is there a possible link between the HABs and nutrient enrichment? These are important points to be addressed in order for the major monitoring programs to help protect marine ecosystems and to secure and support sustainable development, the economy, and the environment of the region.

[23] **Acknowledgments.** This research was supported by INCOIS under the grant (OEC/10-11/102/INCO/PSHA) of the SATCORE program. We would like to thank the NASA SeaWiFS project and all the contributors to the NOMAD database. We would like to thank many scientists who have shared their in situ data in IOCCG database. We gratefully acknowledge Yu-Hwan Ahn and Joo-Hyung Ryu for the KORDI in situ data set. We also gratefully acknowledge C. Hu and J.P. Cannizzaro for the Carder bio-optical data set. The author is indebted to the two anonymous reviewers and E. D. Barton, Editor in Chief, *Journal of Geophysical Research: Oceans*, for their constructive comments and recommendations.

References

Ahn, Y. H., and P. Shanmugam (2006), Detecting red tides from satellite ocean color observations in optically complex Northeast-Asia coastal waters, *Remote Sens. Environ.*, *103*, 419–437, doi:10.1016/j.rse.2006.04.007.

Ahn, Y. H., and P. Shanmugam (2007), Derivation and analysis of the fluorescence algorithms to estimate phytoplankton pigment concentrations in optically complex coastal waters, *J. Opt. A, Pure Appl. Opt.*, *9*, 352–362, doi:10.1088/1464-4258/9/4/008.

Anderson, D. M., P. M. Glibert, and J. M. Burkholder (2002), Harmful algal blooms and eutrophication: Nutrients sources, composition, and consequences, *Estuaries*, *25*, 704–726, doi:10.1007/BF02804901.

Anderson, D. M., B. A. Kefer, W. R. Geyer, R. P. Signell, and T. C. Loder (2005), Toxic *Alexandrium* blooms in the western Gulf of Maine: The "plume advection hypothesis" revisited, *Limnol. Oceanogr.*, *50*, 328–345, doi:10.4319/lo.2005.50.1.0328.

Austin, R. W. (1974), *Inherent Spectral Radiance Signatures of the Ocean Surface. Ocean Color Analysis*, Scripps Inst. of Oceanogr., La Jolla, Calif.

Babin, M., D. Stramski, G.M. Ferrari, H. Claustre, A. Bricaud, G. Obolensky, and N. Hoepffner (2003), Variations in the light absorption coefficients of phytoplankton, nonalgal particles, and dissolved organic matter in coastal waters around Europe, *J. Geophys. Res.*, *108*(C7), 3211, doi:10.1029/2001JC000882.

Bailey, S. W., and P. J. Werdell (2006), A multi-sensor approach for the on-orbit validation of ocean color satellite data products, *Remote Sens. Environ.*, *102*, 12–23, doi:10.1016/j.rse.2006.01.015.

Bailey, S. W., B. A. Franz, and P. J. Werdell (2010), Updated NIR water-leaving radiance estimation for ocean color data processing, *Opt. Express*, *18*, 7521–7527, doi:10.1364/OE.18.007521.

Behrenfeld, M. J., and P. G. Falkowski (1997), Photosynthetic rates derived from satellite-based chlorophyll concentration, *Limnol. Oceanogr.*, *42*, 1–20, doi:10.4319/lo.1997.42.1.0001.

Brand, L. E., and A. Compton (2007), Long-term increase in Karenia brevis abundance along the southwest Florida Coast, *Harmful Algae*, *6*, 232–252, doi:10.1016/j.hal.2006.08.005.

Bricaud, A., A. Morel, M. Babin, K. Allali, and H. Claustre (1998), Variations of light absorption by suspended particles with chlorophyll *a* concentration in oceanic (case 1) waters: Analysis and implications for bio-optical models, *J. Geophys. Res.*, *103*, 31,033–31,044, doi:10.1029/98JC02712.

Campbell, J. W., and W. E. Esaias (1983), Basis for spectral curvature algorithms in remote sensing of chlorophyll, *Appl. Opt.*, *22*, 1084–1093, doi:10.1364/AO.22.001084.

Cannizzaro, J. P., K. L. Carder, F. R. Chen, C. A. Heil, and G. A. Vargo (2008), A novel technique for detection of the toxic dinoflagellate *Karenia brevis* in the Gulf of Mexico from remotely sensed ocean color data, *Cont. Shelf Res.*, *28*, 137–158, doi:10.1016/j.csr.2004.04.007.

Cannizzaro, J. P., C. Hu, D. C. English, K. L. Carder, C. A. Heil, and F. E. Muller-Karger (2009), Detection of *Karenia brevis* blooms on the west Florida shelf using in situ backscattering and fluorescence data, *Harmful Algae*, *8*, 898–909, doi:10.1016/j.hal.2009.05.001.

Carder, K. L., and R. G. Steward (1985), A remote-sensing reflectance model of a red-tide dinoflagellate off west Florida, *Limnol. Oceanogr.*, *30*, 286–298, doi:10.4319/lo.1985.30.2.0286.

Carder, K. L., F. R. Chen, Z. P. Lee, S. K. Hawes, and D. Kamykowski (1999), Semi-analytic Moderate-Resolution Imaging Spectrometer algorithms for chlorophyll *a* and absorption with bio-optical domains based on nitrate-depletion temperatures, *J. Geophys. Res.*, *104*, 5403–5421, doi:10.1029/1998JC900082.

Carstensen, J., D. J. Conley, and P. Henriksen (2004), Frequency, composition, and causes of summer phytoplankton blooms in a shallow coastal ecosystem, the Kattegat, *Limnol. Oceanogr.*, *49*, 191–201, doi:10.4319/lo.2004.49.1.0191.

Chauhan, P., M. Mohan, R. K. Sarngi, B. Kumari, S. Nayak, and S. G. Matondkar (2002), Surface chlorophyll *a* estimation in the Arabian Sea using IRS-P4 Ocean Colour Monitor (OCM) satellite data, *Int. J. Remote Sens.*, *23*(8), 1663–1676, doi:10.1080/01431160110075866.

Cullen, J. J., A. M. Ciotti, R. F. Davis, and M. R. Lewis (1997), Optical detection and assessment of algal blooms, *Limnol. Oceanogr.*, *42*, 1223–1239, doi:10.4319/lo.1997.42.5_part_2.1223.

Darecki, M., and D. Stramski (2004), An evaluation of MODIS and SeaWiFS bio-optical algorithms in the Baltic Sea, *Remote Sens. Environ.*, *89*, 326–350, doi:10.1016/j.rse.2003.10.012.

Desa, E., T. Suresh, S. G. P. Matondkar, and E. Desa (2001), Sea truth validation of SeaWiFS ocean colour sensor in the coastal waters of the Eastern Arabian Sea, *Curr. Sci.*, *80*(7), 854–860.

Edwards, M., D. G. Johns, S. C. Leterme, E. Svendsen, and A. J. Richardson (2006), Regional climate change and harmful algal blooms in the northeast Atlantic, *Limnol. Oceanogr.*, *51*, 820–829, doi:10.4319/lo.2006.51.2.0820.

Emmett Duffy, J. (2011), Arabian Sea large marine ecosystem, in *Encyclopedia of Earth* [electronic], edited by C. J. Cleveland, Environ. Inf. Coalition, Natl. Counc. for Sci. and the Environ., Washington, D. C. [Available at http://www.eoearth.org/article/Arabian_Sea_large_marine_ecosystem.]

Garcia, C. A. E., V. M. T. Garcia, and C. R. McClain (2005), Evaluation of SeaWiFS chlorophyll algorithms in the southwestern Atlantic and Southern oceans, *Remote Sens. Environ.*, *95*, 125–137, doi:10.1016/j.rse.2004.12.006.

Goes, J. I., P. G. Thoppil, H. R. Gomes, and J. T. Fasullo (2005), Warming of the Eurasian landmass is making the Arabian Sea more productive, *Science*, *308*, 545–547, doi:10.1126/science.1106610.

Gomes, H. R., J. I. Goes, S. G. P. Matondkar, S. G. Parab, A. R. N. Al-Azri, and P. G. Thoppil (2008), Blooms of *Noctiluca miliaris* in the Arabian Sea—An in situ and satellite study, *Deep Sea Res. Part I*, *55*, 751–765, doi:10.1016/j.dsr.2008.03.003.

Gordon, H. R., and A. Morel (1983), Remote assessment of ocean color for interpretation of satellite visible imagery—A review, in *Lecture Notes on Coastal and Estuarine Studies*, edited by R. T. Barber et al., pp. 1–144, Springer, New York.

Gordon, H. R., and M. Wang (1994), Retrieval of water-leaving radiance and aerosol optical thickness over the oceans with SeaWiFS: A preliminary algorithm, *Appl. Opt.*, *33*, 443–452, doi:10.1364/AO.33.000443.

Gordon, H. R., O. B. Brown, R. H. Evans, J. W. Brown, R. C. Smith, K. S. Baker, and D. K. Clark (1988), A semianalytic radiance model of ocean color, *J. Geophys. Res.*, *93*, 10,909–10,924, doi:10.1029/JD093iD09p10909.

Gower, J. F. R., and G. A. Borstad (1990), Mapping of phytoplankton by solar-stimulated fluorescence using an imaging spectrometer, *Int. J. Remote Sens.*, *11*(2), 313–320, doi:10.1080/01431169008955022.

Harding, L. W., Jr., E. C. Itsweire, and W. E. Esaias (1992), Determination of phytoplankton chlorophyll concentrations in the Chesapeake Bay with aircraft remote sensing, *Remote Sens. Environ.*, *40*, 79–100, doi:10.1016/0034-4257(92)90007-7.

Hu, C., F. E. Muller-Karger, C. J. Taylor, K. L. Carder, C. Kelble, E. Johns, and C. A. Heil (2005), Red tide detection and tracing using MODIS fluorescence data: A regional example in SW Florida coastal waters, *Remote Sens. Environ.*, *97*, 311–321, doi:10.1016/j.rse.2005.05.013.

Joint Global Ocean Flux Study (2002), *Indian Ocean Synthesis Group on the Arabian Sea Process Study*, edited by L. Watts, P. Burkill, and S. Smith, Bergen, Norway.

Kirk, J. T. O. (1994), *Light and Phytosynthesis in Aquatic Ecosystems*, 2nd ed., doi:10.1017/CBO9780511623370, Cambridge Univ. Press, New York.

Kirkpatrick, B., et al. (2004), Literature review of Florida red tide: Implications for human health effects, *Harmful Algae*, *3*, 99–115, doi:10.1016/j.hal.2003.08.005.

Kostadinov, T. S., D. A. Siegel, S. Maritorena, and N. Guillocheau (2007), Ocean color observations and modeling for an optically complex site: Santa Barbara Channel, California, USA, *J. Geophys. Res.*, *112*, C07011, doi:10.1029/2006JC003526.

Kutser, T., L. Metsamaa, N. Strombeck, and E. Vahtma (2006), Monitoring cyanobacterial blooms by satellite remote sensing, *Estuarine Coastal Shelf Sci.*, *67*, 303–312, doi:10.1016/j.ecss.2005.11.024.

Lee, Z. (Ed.) (2006), Remote sensing of inherent optical properties: Fundamentals, tests of algorithms and applications, 126 pp., Int. Ocean-Color Coord. Group Proj. Off., Dartmouth, N. S., Canada.

Marrari, M., C. Hu, and K. Daly (2006), Validation of SeaWiFS chlorophyll *a* concentrations in the Southern Ocean: A revisit, *Remote Sens. Environ.*, *105*, 367–375, doi:10.1016/j.rse.2006.07.008.

Martin Traykovski, L. V., and H. M. Sosi (2003), Feature-based classification of optical water types in the Northwest Atlantic based on satellite ocean color data, *J. Geophys. Res.*, *108*(C5), 3150, doi:10.1029/2001JC001172.

Mobley, C. D. (1994), *Light and Water: Radiative Transfer in Natural Waters*, 592 pp., Elsevier, New York.

Morel, A., and L. Prieur (1977), Analysis of variations in ocean color, *Limnol. Oceanogr.*, *22*, 709–722, doi:10.4319/lo.1977.22.4.0709.

O'Reilly, J. E., S. Maritorena, B. G. Mitchell, D. A. Siegel, K. L. Carder, S. A. Garver, M. Kahru, and C. McClain (1998), Ocean color algorithms for SeaWiFS, *J. Geophys. Res.*, *103*, 24,937–24,953, doi:10.1029/98JC02160.

O'Reilly, J. E., et al. (2000), Ocean color chlorophyll *a* algorithms for SeaWiFS, OC2, and OC4: Version 4, in *SeaWiFS Postlaunch Calibration and Validation Analyses*, *Part 3*, *SeaWiFS Postlaunch Tech. Rep. Ser.*, vol. 11, edited by S. B. Hooker and E. R. Firestone, pp. 9–23, NASA Goddard Space Flight Cent., Greenbelt, Md.

Otero, M., and D. A. Siegel (2004), Spatial and temporal characteristics of sediment plumes and phytoplankton blooms in the Santa Barbara Channel, *Deep Sea Res. Part II*, *51*, 1129–1149.

Pan, X., A. Mannino, M. E. Russ, and S. B. Hooker (2008), Remote sensing of the absorption coefficients and chlorophyll a concentration in the United States southern Middle Atlantic Bight from SeaWiFS and MODIS-Aqua, *J. Geophys. Res.*, *113*, C11022, doi:10.1029/2008JC004852.

Sathyendranath, S. (Ed.) (2000), Remote sensing of ocean colour in coastal, and other optically complex, waters, *Int. Ocean-Color Coord. Group Rep. 3*, Int. Ocean-Color Coord. Group Proj. Off., Dartmouth, N. S., Canada.

Schofield, O., J. Grzymski, W. P. Bissett, G. J. Kirkpatrick, D. F. Millie, M. Moline, and C. S. Roesler (1999), Optical monitoring and forecasting systems for harmful algal blooms: Possibility or pipe dream?, *J. Phycol.*, *35*, 1477–1496, doi:10.1046/j.1529-8817.1999.3561477.x.

Schofield, O., T. Bergmann, W. P. Bissett, M. A. Moline, and C. Orrico (2004), Inverting inherent optical signatures in the near shore coastal waters at the Long Term Ecosystem Observatory, *J. Geophys. Res.*, *109*, C12S04, doi:10.1029/2003JC002071.

Sellner, K. G., G. J. Doucette, and G. J. Kirkpatrick (2003), Harmful algal blooms: Causes, impacts and detection, *J. Ind. Microbiol. Biotechnol.*, *30*, 383–406, doi:10.1007/s10295-003-0074-9.

Shanmugam, P. (2010), SeaDAS atmospheric correction algorithm to improve retrievals of surface reflectance in Case 2 waters, paper presented at Ocean Optics XX, Oceanogr. Soc., Anchorage, Alaska, 25 Sept. to 1 Oct.

Shanmugam, P., Y. H. Ahn, and P. S. Ram (2008), SeaWiFS sensing of hazardous algal blooms and their underlying mechanisms in shelf-slope waters of the Northwest Pacific during summer, *Remote Sens. Environ.*, *112*, 3248–3270, doi:10.1016/j.rse.2008.04.002.

Siegel, D. A., M. C. O'Brien, J. C. Sorensen, D. A. Konnoff, and E. Fields (1995), *U.S. JGOFS—BBOP Data Processing and Sampling Procedures, ICESS*, Univ. of Calif. Press, Santa Barbara, Calif.

Siegel, D. A., M. Wang, S. Maritorena, and W. Robinson (2000), Atmospheric correction of satellite ocean color imagery: The black pixel assumption, *Appl. Opt.*, *39*, 3582–3591, doi:10.1364/AO.39.003582.

Siegel, D. A., S. Maritorena, N. B. Nelson, D. A. Hansell, and M. Lorenzi-Kayser (2002), Global distribution and dynamics of colored dissolved and detrital organic materials, *J. Geophys. Res.*, *107*(C12), 3228, doi:10.1029/2001JC000965.

Steidinger, K. A., and K. Haddad (1981), Biologic and hydrographic aspects of red tides, *BioScience*, *31*, 814–819, doi:10.2307/1308678.

Stramska, M., D. Stramski, R. Hapter, S. Kaczmarek, and J. Stoń (2003), Bio-optical relationships and ocean color algorithms for the north polar region of the Atlantic, *J. Geophys. Res.*, *108*(C5), 3143, doi:10.1029/2001JC001195.

Stumpf, R. P. (2001), Applications of satellite ocean color sensors for monitoring and predicting harmful algal blooms, *Hum. Ecol. Risk Assess.*, *7*, 1363–1368, doi:10.1080/20018091095050.

Stumpf, R. P., et al. (2003), Monitoring *Karenia brevis* blooms in the Gulf of Mexico using satellite ocean color imagery and other data, *Harmful Algae*, *2*, 147–160.

Subramaniam, A., C. W. Brown, R. R. Hood, E. J. Carpenter, and D. G. Capone (2001), Detecting *Trichodesmium* blooms in SeaWiFS imagery, *Deep Sea Res. Part II*, *49*, 107–121, doi:10.1016/S0967-0645(01)00096-0.

Tang, D. L., H. Kawamura, and A. J. Luis (2002), Short-term variability of phytoplankton blooms associated with a cold eddy in the northwestern Arabian Sea, *Remote Sens. Environ.*, *81*, 82–89, doi:10.1016/S0034-4257(01)00334-0.

Tomlinson, M. C., et al. (2004), Evaluation of the use of SeaWiFS imagery for detecting Karenia brevis harmful algal blooms in the eastern Gulf of Mexico, *Remote Sens. Environ.*, *91*, 293–303, doi:10.1016/j.rse.2004.02.014.

Volpe, G., R. Santoleri, V. Vellucci, D. M. Ribera d'Alcalà, S. Marullo, and F. D'Ortenzio (2007), The colour of the Mediterranean Sea: Global versus regional bio-optical algorithms evaluation and implication for satellite chlorophyll estimates, *Remote Sens. Environ.*, *107*, 625–638, doi:10.1016/j.rse.2006.10.017.

Walsh, J. J., et al. (2006), Red tides in the Gulf of Mexico: Where, when, and why?, *J. Geophys. Res.*, *111*, C11003, doi:10.1029/2004JC002813.

Wang, M., and W. Shi (2005), Estimation of ocean contribution at the MODIS near-infrared wavelengths along the east coast of the U.S.: Two case studies, *Geophys. Res. Lett.*, *32*, L13606, doi:10.1029/2005GL022917.

Westberry, T. K., D. A. Siegel, and A. Subramaniam (2005), An improved bio-optical model for the remote sensing of *Trichodesmium spp*. Blooms, *J. Geophys. Res.*, *110*, C06012, doi:10.1029/2004JC002517.

Wynne, T. T., R. P. Stumpf, M. C. Tomlinson, V. Ransibrahmanakul, and T. A. Villareal (2005), Detecting *Karenia brevis* blooms and algal resuspension in the western Gulf of Mexico with satellite ocean color imagery, *Harmful Algae*, *4*, 992–1003, doi:10.1016/j.hal.2005.02.004.

Yentsch, C. S., B. E. Lapointe, N. Poulton, and D. A. Phinney (2008), Anatomy of a red tide bloom off the southwest coast of Florida, *Harmful Algae*, *7*, 817–826, doi:10.1016/j.hal.2008.04.008.

P. Shanmugam, Ocean Optics and Imaging Group, Department of Ocean Engineering, Indian Institute of Technology Madras, Chennai 600036, India. (pshanmugam@iitm.ac.in)